Hew, *Planta* 132, 303 (1975); H. Griffiths and J. A. C. Smith, *Oecologia* 60, 176 (1983).
7. P. W. Richards, *The Tropical Rain Forest* (Cambridge Univ. Press, Cambridge, 1964).
8. D. F. Parkhurst, *Am. J. Bot.* 69, 31 (1982).
9. D. W. Northfelt, M. J. DeNiro, S. Epstein, *Geochim. Cosmochim. Acta* 45, 1895 (1981).
10. The carbon isotope ratios are expressed in the δ notation, where

$$\delta^{13}C = \frac{R_{sample}}{R_{standard}} - 1 \times 100 \text{ per mil}$$

where R represents the $^{13}C/^{12}C$ ratio and the standard is the Pee Dee belemnite carbonate. The precision of the determinations of $\delta^{13}C$ values, based on replicate analyses of individual samples, was ±0.2 per mil.
11. G. S. Byott, *N. Phytol.* 76, 295 (1976).
12. R. D. Warmbrodt, *Am. J. Bot.* 71, 330 (1984).
13. J. A. C. Smith and S. Heuer, *Ann. Bot.* 48, 915 (1981).
14. C. Tinoco Ojanguren and C. Vazquez-Yanes, *Bol. Soc. Bot. Mex.* 45, 150 (1983).
15. The field research was conducted during a University of California Research Expeditions Program to the U.S. Virgin Islands in July 1984. Participants were M. Becker, J. Brandenberger, L. Johnson, L. Labos-Simpao, S. McMahon, L. Poli, and J. Simmons. We thank the National Park Service, Virgin Islands National Park, Saint Thomas, for allowing us to work in the national park on Saint John. We also thank J. Hann for assistance in the laboratory at Riverside and H. Ajie and D. Winter for assistance in determining the $\delta^{13}C$ values. Supported by NSF grants PCM82-00366 (I.P.T.), DBM84-05003 (M.J.D.), and PCM 8303-619 (E.M.L.).

7 February 1985; accepted 2 July 1985

caya ice cap is unusual. Previous temperature measurements to a depth of 37.5 m suggested that Quelccaya is temperate–that is, the ice is at the pressure melting point (0.0°C). However, from 42.5 to 160 m in the core, between 0.5 and 0.8 cm of new bubble-free ice would freeze at the bottom of the borehole overnight. Both boreholes contained meltwater derived in part from the temperate upper layer of the ice cap and in part from the use of a thermal drill. Thermodynamic calculations indicate that ice temperature between 42.5 and 160 m must be 1° to 3°C below the pressure melting point.

Three representative core sections (Fig. 1) show the distinct annual dust layers used to date these cores and the thinning of annual layers occurring with depth. Annual-layer thickness (ice equivalent) ranges from 1.2 m at the surface to 0.01 m at the base. The time scale, based solely on visible dust layers, is subject to errors in the upper firn sections, where the core is not transparent and dust layers are more difficult to see. Additionally, annual layers may be missed when the visible dust band is thin and occurs where the core is broken into sections during drilling. Individual core sections were 2 m in length and 8 cm in diameter on average. Selected core sections were analyzed in the field for both liquid and solid conductivity. Six thousand samples were collected for microparticle and oxygen-isotope analyses, and 1500 samples for total beta radioactivity and chemical measurements.

Little is known about the relation between tropical glaciers and long-term variations in tropical climate. Quelccaya (latitude 13°56'S, longitude 70°50'W), in the outer tropics on the western margin of the Amazon Basin, is located in a climatically sensitive region (*5*). The annual mean temperature at this high ice cap (elevation 5670 m) is −3°C, precluding significant melting and percolation. The 55-km^2 ice cap sits on an extensive and relatively flat ignimbrite plateau, with simple radial flow causing little distortion of the ice layers (*1*, *6*).

Snow pits and shallow ice cores have been sampled each year since 1976 to determine seasonal variations in microparticles, oxygen isotopes, and beta radioactivity (*1*, *7*). Automatic weather stations (RIMCO Mark III) have provided records of temperature, wind speed and direction, and sunshine duration for periods extending from 3 to 8 months each year since 1976. These data, although incomplete, provide a link between the meteorological conditions on Quelccaya

A 1500-Year Record of Tropical Precipitation in Ice Cores from the Quelccaya Ice Cap, Peru

Abstract. *Two ice cores, covering 1500 years of climatic information, from the summit (5670 meters) of the tropical Quelccaya ice cap, in the Andes of southern Peru, provide information on general environmental conditions including droughts, volcanic activity, moisture sources, temperature, and glacier net balance. The net balance record reconstructed from these cores reflects major precipitation trends for the southern Andes of Peru. These records indicate extended dry periods between 1720 and 1860, 1250 and 1310, and 570 and 610; wet conditions prevailed between 1500 and 1720. Establishing a tropical precipitation record may help explain climatic fluctuations since the tropical evaporation-precipitation cycle is a principal mechanism driving the atmospheric circulation.*

L. G. Thompson
E. Mosley-Thompson
J. F. Bolzan
Institute of Polar Studies, Ohio State University, Columbus 43210
B. R. Koci
Polar Ice Coring Office, University of Nebraska, Lincoln 68588-0200

Since 1976 a glaciological research program (*1*) has been conducted each summer on the tropical Quelccaya ice cap in the Andes of southern Peru. In 1983 two cores were recovered, one 154.8 m long with 1350 years of climatic information and the other 163.6 m long with 1500 years. Visibly distinct annual dust layers (Fig. 1) made it possible to date these cores accurately. Because the site is too remote and too high for the use of a conventional drill system, a newly designed portable light-weight, solar-powered drill was used (*2*).

A mono-pulse radar unit (*3*, *4*), was used to determine ice thickness (Fig. 2). The 163.6-m core (core 1) was drilled to bedrock and the 154.8-m core (summit core) was drilled to some undetermined distance above the bedrock after penetration of an unconformity at 153.7 m (Fig. 2). This unconformity consisted of dust layers inclined 18° from the horizontal and contained elongated air bubbles just above two distinct bubble-free ice layers, one 13 cm thick and the other 8 cm thick. Below the bubble-free ice, the distinct annual dust layers were horizontal with round air bubbles. The unconformity may represent a shear zone between stagnant ice in the depression (Fig. 2) just east of the summit and the upper active ice. Therefore, core 1 is considered the better record before A.D. 1200 because it is continuous from the surface to bedrock. The bedrock is relatively flat at the core 1 site and all the visible dust layers were horizontal from top to bottom.

The temperature profile for the Quelc-

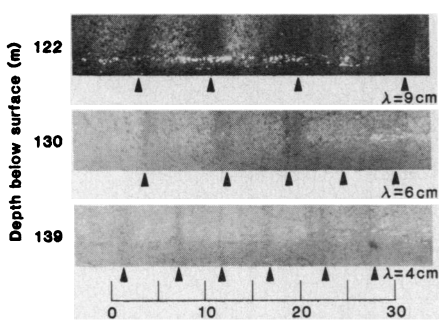

Fig. 1. Three representative core sections show the distinct annual dry season dust layers (triangles) used to date the cores. The average thickness (λ) of the annual layers is shown; annual layer thinning with depth is evident (see Fig. 4).

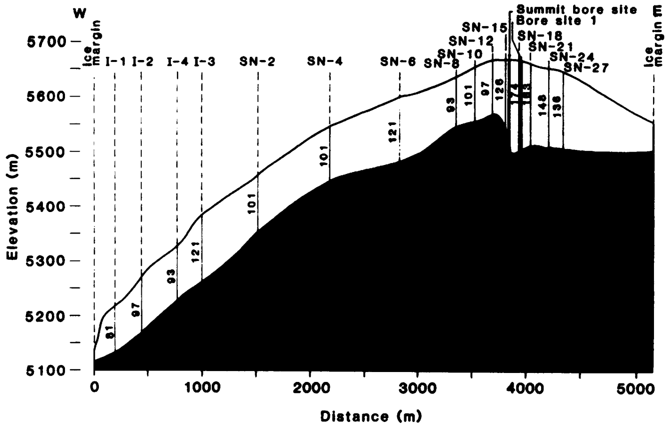

Fig. 2. Ice-cap thickness along an east-west traverse calculated from monopulse radar data.

and those recorded for the same period at surrounding meteorological stations.

Surface heat-budget studies, including lysimetric measurements and bulkaerodynamic estimates, based on data collected during the dry ablation period (May through September), indicate that there is essentially no energy available for evaporation and melting (*7, 8*). Under current meteorological conditions the thickness of the layer accumulating at the summit each year should reflect the regional precipitation. Therefore the 1500-year net balance record reconstructed from these ice cores provides a well-dated precipitation history with excellent temporal resolution (annual to decadal resolution) for southern Peru.

Although the thickness of annual layers can be measured throughout both cores, the layers do not directly represent the thickness originally deposited at the ice-cap surface. Because these layers are thinned and stretched as new snow accumulates and the ice flows outward from the center (Fig. 3), the thinning of each layer with time must be taken into account.

The rate of thinning can be calculated if the vertical strain rate $\dot{e}_z(t)$ is known as a function of time (*9*). Let L_{0i} be the initial thickness of the *i*th layer, deposited at the surface. The corresponding layer thickness at some later time t_i (when the layer is buried to depth z_i) may be expressed as

$$L(t_i) = L_{0i} \exp\left[\int_0^{t_i} \dot{e}_z(t)dt\right] \quad (1)$$

where the vertical strain rate per year is equivalent to the fractional change in layer thickness per year. The vertical strain rate in Eq. 1 is time-dependent for two reasons. First, the stresses causing deformation usually vary with depth in the ice sheet, giving rise to depth-dependent strain rates. Thus as a layer is buried to depth z it experiences a deformation rate that varies with time. Second, changes in accumulation cause changes in stress, velocity, and ice thickness that produce a time-dependent vertical strain rate distribution at a given depth as the ice cap re-equilibrates. To simplify the calculation, it is assumed that the vertical strain rate at a given depth is independent of time—that is, a steady-state condition is assumed for the last 1500 years. This assumption is reasonable if the derived net balance changes by only a relatively small amount.

The vertical strain rate profile in a borehole is difficult to measure directly but may be estimated from the flow law for ice, if the stress distribution can be specified. In an earlier study (*3*), the age of the ice as a function of depth was calculated assuming the longitudinal deviator stress to vary linearly with depth; Glen's flow law (with $n = 3$) was used to calculate the longitudinal strain rate. Here the measured layer thicknesses are used to calculate the vertical strain rate profile. If the ice cap were in steady-state, changes in layer thickness with depth would result entirely from deformation. Let $L(t)$ be the layer thickness at time t when the layer has been buried to depth z, and let $L(t + dt)$ be the layer thickness at some later time. The average vertical strain rate over the time interval t to $(t + dt)$ is defined as

$$\dot{e}_z(t) = [L(t + dt) - L(t)]/L(t)dt \quad (2)$$

where dt is 1 year. Successive layers may vary greatly in thickness because of secular net balance variations, and thus an average layer thickness is defined for N layers as

$$\bar{L}(t_i) = (1/N)\sum_j L(t_j) \quad (3)$$

where $\bar{L}(t_j)$ is summed from $j = i - (N/2)$ to $j = i + (N/2)$. If N is large, the stochastic variations in net balance should average out. The vertical strain rate is then calculated as a function of time from Eq. 2, with M-N values generated where M is the number of layers in either core. Further smoothing of the calculated vertical strain rate is obtained by fitting $\dot{e}_z(t)$ with a simple nth order polynomial.

$$\dot{e}_z(t) = \sum_{i=0}^{n} c_i t^i \quad (4)$$

This strain-rate function is then substituted into Eq. 1 to calculate the initial layer thickness, L_{0i}, from the measured $L(t_i)$.

There is some ambiguity in this approach, as the values of the reconstructed net balances depend on the values of N (Eq. 3) and n (Eq. 4). To resolve this, two additional constraints are imposed. First the average net balance during the past 1280 years (the record above the summit-core unconformity) is assumed to be the same in both cores. Recent surface measurements indicate similar net balances for both core sites, separated by about 150 m. Second, the surface vertical strain rate (the strain rate at $t = 0$) given by the nth order polynomial must match the vertical strain rate measured at each borehole site. Measurements of the deformation of a strain grid in 1984 give 1.91×10^{-2} per year and 1.45×10^{-2} per year for the surface vertical strain rate in the vicinity of core 1 and summit borehole sites, respectively. Both requirements are satisfied with $N = 40$ and $n = 4$ for core 1 and $N = 20$ and $n = 4$ for the summit core.

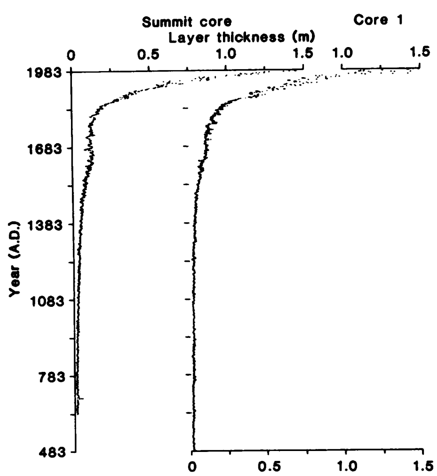

Fig. 3. Five-year weighted running means for the measured annual layer thickness for both ice cores. The thick layer at 684 in the summit core is due to an unconformity in the annual layer sequence.

Qualitative trends in the reconstructed 10-year-averaged net balances for both cores (Fig. 4) are in excellent agreement, even in the lower part of the record, where the detailed deformation history becomes increasingly important. A prominent feature is the drought from 1720 to 1860 A.D., also evident in the measured layer thickness (Fig. 3). Several simple analytic forms for the depth-dependent vertical strain rate were considered. The net balance profiles are similar in all these reconstructions, although the intensity of the wet and dry periods is model-dependent. This suggests that in the more recent part of the record, the reconstructed qualitative long-term trends in net balance are relatively insensitive to the detailed form of the vertical strain rate.

There are short-term (annual to decadal) variations in net balance between the two cores (Fig. 4). Postdepositional processes can alter the original layer thickness, introducing considerable spatial variability, although under present conditions this seems insignificant. Deep in the cores, where layers are only a few centimeters thick, measurement errors may create substantial differences between the two cores for identical annual units. The short-term differences may also partially result from errors in the annual assignment of the layers.

This reconstructed net balance record represents a complex integration of local and large-scale climate variations. The wet season typically extends from November to April when the sun is nearly overhead. The high Peruvian-Bolivian altiplano, as well as the lower atmosphere, are heated by intense solar radiation before noon while cloudiness is minimal. At lower levels relatively moist air masses are advected from the east and northeast, producing intense convection and precipitation predominantly in the afternoon (*10*). A continental heat low forms over Gran Chaco and the Pampean Sierras, producing monsoonal convergent low-level flow from the moisture-rich Amazon Basin which contributes significantly to the formation of persistant, intense convection during the Southern Hemisphere summer (*11*). To the south and west along the axis of the Andes, a greater proportion of the annual total precipitation falls in the wet season which accounts for approximately 80 percent of the annual precipitation in the area of Quelccaya (*12*). This seasonality of precipitation leads to the distinct annual stratigraphy preserved in the ice.

Both Quelccaya net balance records (Fig. 4) show similar trends (Table 1). A period of maximum drought from 1720 to 1860 followed a pluvial period from 1500 to 1720. During the most recent neoglacial or Little Ice Age of the Northern Hemisphere, the Quelccaya ice cap was larger as indicated by terminal moraines (*13*) radiocarbon dated to 1500 ± 200 years. This ice cap advance may have been a response to the increased precipitation (1500 to 1720) and associated reduction in radiation (increased cloudiness). Net balance records indicate a dry period between 1160 and 1500, that was especially intense between 1250 and 1310. The curves for the two cores are not well matched before about 1160 because of nonuniform errors in the field measurements of annual-layer separations for the two cores (Fig. 4) and the increasing importance of deformation history. Because core 1 net balance trends before 1200 are considered more reliable, the wet and dry intervals before 1200 (Table 1) are inferred only from core 1.

Table 1. Precipitation trends from the Quelccaya ice cores.

Wetter periods	Drier periods
1870–1984	1720–1860*
1500–1720*	1250–1310*
760–1040	650–730
610–650	570–610*
	540–560

*Extremes—periods for which average precipitation for both cores is 20 percent higher or lower than the mean.

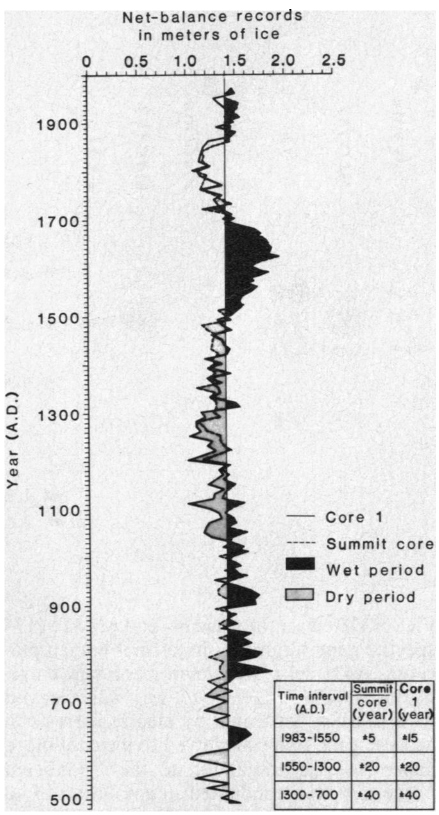

Fig. 4. The 10-year average of the reconstructed net balance record of both ice cores. The vertical line represents the average accumulation for both cores. The potential errors (table inset) between 1983 and 1550 were determined for each core as the differences between the time scale derived from the annual microparticle and $\delta^{18}O$ signals and that based on the visible stratigraphy. The potential errors before 1550 represent the age differences between identical microparticle and $\delta^{18}O$ features readily identified in both cores.

Ice caps and sheets are excellent storage systems for past atmospheric conditions. Tropical ice caps, which contain physical and chemical records and distinct annual layers for accurate dating, are rare. The two Quelccaya ice cores provide a high-resolution (annual to decadal) proxy record of tropical precipitation. This record, in conjunction with microparticles, oxygen isotopes, conductivity, and pollen distributions, will provide additional information about the physical environment in southern Peru over the last 1500 years. Integration of all these records, as well as refinement of the time scales by use of annual signals in microparticles and oxygen isotopes, may help isolate the principal mechanisms responsible for these climatic fluctuations.

References and Notes

1. L. G. Thompson, E. Mosley-Thompson, P. M. Grootes, M. Pourchet, S. Hastenrath, *J. Geophys. Res.* **89**, 4638 (1984).
2. The drill system consisted of 48 solar panels which provided an average of 1200 W and produced drilling rates of 3 m per hour. A lightweight portable winch and cable along with an electromechanical drill were used in the upper 30 m, and a thermal drill was used from 30 m to bedrock. This was the first use of solar power in a major ice coring effort.
3. L. G. Thompson, J. F. Bolzan, H. H. Brecher, P. D. Kruss, E. Mosley-Thompson, K. C. Jezek, *J. Glaciol.* **28**, 57 (1982).
4. K. C. Jezek and L. G. Thompson, *IEEE Trans. Geosci. Remote Sens.* **GE-10**, 243 (1982).
5. L. G. Thompson, E. Mosley-Thompson, B. Morales Arnao, *Science* **226**, 50 (1984).
6. L. G. Thompson, *J. Glaciol.* **25**, 69 (1980).
7. ______, S. Hastenrath, B. Morales Arnao, *Science* **203**, 1240 (1979).
8. S. Hastenrath, *J. Glaciol.* **20**, 85 (1978).
9. C. H. Hammer, H. B. Clausen, W. Dansgaard, N. Gundestrup, S. J. Johnson, N. Reeh, *ibid.*, p. 3; I. M. Whillans, *ibid.* **24**, 15 (1979); W. S. B. Paterson and E. D. Waddington, *Rev. Geophys. Space Phys.* **22**, 123 (1984).
10. G. Gutman and W. S. Schwerdtfeger, *Meteorol. Rundsch.* **18** (No. 3), 1 (1965).
11. H. Virji, thesis, University of Wisconsin, Madison (1979), p. 93.
12. A. M. Johnson, *World Survey of Climatology, Climates of Central and South America*, W. Schwerdtfeger, Ed. (Elsevier, Amsterdam, 1976), vol. 12, p. 147.
13. J. H. Mercer and O. M. Palacios, *Geology* **5**, 600 (1977); J. H. Mercer, in *Proceedings of the International Symposium on Late Cainozoic, Paleoclimates of the Southern Hemisphere*, J. C. Vogel, Ed. (Balkema, Rotterdam, in press).
14. Supported by NSF grants ATM75-15513A02, ATM7821609A01, ATM-8105079A02, and ATM8213601A01. The NSF Division of Polar Programs supported 1974 field investigations (GV41411) and development of the solar-powered drill. We thank B. Morales Arnao as well as numerous scientists, engineers, and technicians from Electroperu (Lima and Huaraz offices) for scientific and logistical assistance. We also thank W. Berk and the Inter-American Geodetic Survey (U.S. Defense Mapping Agency) office in Lima for logistical support. Many people have participated in the ten field programs, and their efforts are gratefully acknowledged, especially those of the 1983 expedition, E. Angeles, C. Chadwell, S. Hastenrath, B. Koci, P. Kruss, K. Mountain, M. Strobel, F. Vicencio, and M. Zamora. We thank M. Davis for assistance in the laboratory analysis and R. Tope for the illustrations. Contribution 527 of the Institute of Polar Studies, Ohio State University.

26 December 1984; accepted 13 June 1985